Chapter 4

Nuclear Uptake of Polyamide-Fluorophore Conjugates in Mammalian Cell Lines

Chapter 4A: *The text of this chapter was taken in part from a manuscript coauthored with Benjamin S. Edelson, Nicholas G. Nickols, and Professor Peter B. Dervan (Caltech).*

(Best, T.P.; Edelson, B.S.; Nickols, N.G.; Dervan, P.B. "Nuclear Localization of Pyrrole-Imidazole Polyamide-Fluorescein Conjugates in Cell Culture" *Proc. Natl. Acad. Sci. U.S.A.* **2003**, *100*, 12063.)

Chapter 4B: *The text of this chapter was taken in part from a manuscript coauthored with Benjamin S. Edelson, Bogdan Olenyuk, Nicholas G. Nickols, Raymond M. Doss, Shane Foister, Alexander Heckel, and Professor Peter B. Dervan (Caltech).*

(Edelson, B.S.; Best, T.P.; Olenyuk, B.; Nickols, N.G.; Doss, R.M.; Foister, S.; Heckel, A.; Dervan, P.B. "Influence of Structural Variation on Nuclear Localization of DNA-Binding Polyamide-Fluorophore Conjugates" *Nuc. Acids Res.* **2004**, *32*, 2802.)

Chapter 4A

Polyamide-FITC Conjugates for Cellular Uptake Studies

Abstract

A series of hairpin pyrrole-imidazole polyamide-fluorescein conjugates were synthesized and assayed for cellular localization. Thirteen cell lines, representing eleven human cancers, one human transformed kidney cell line, and one murine leukemia cell line, were treated with 5 μM polyamide-fluorescein conjugates for 10-14 hrs, then imaged by confocal laser scanning microscopy. A conjugate containing a β-alanine residue at the C-terminus of the polyamide moiety showed no nuclear localization, while an analogous compound lacking the β-alanine residue was strongly localized in the nuclei of all cell lines tested. The localization profiles of several other conjugates suggest that pyrrole-imidazole sequence and content, dye choice and position, linker composition, and molecular weight are determinants of nuclear localization. The attachment of fluorescein to the C-terminus of a hairpin polyamide results in an approximate 10-fold reduction in DNA-binding affinity, with no loss of binding specificity with reference to mismatch binding sites.

Introduction

Small molecules that preferentially bind to predetermined DNA sequences inside living cells would be useful tools in molecular biology, and perhaps human medicine. The effectiveness of these small molecules requires not only that they bind to chromosomal DNA site-specifically, but also that they be permeable to the outer membrane and gain access to the nucleus of living cells. Polyamides containing the aromatic amino acids *N*-methylpyrrole (Py), *N*-methylimidazole (Im) and *N*-methyl-3-hydroxypyrrole (Hp) bind DNA with affinities and specificities comparable to naturally occurring DNA-binding proteins.[1,2] A set of pairing rules describes the interactions between pairs of these heterocyclic rings and Watson-Crick base pairs within the minor groove: Im/Py is specific for G•C, Hp/Py is specific for T•A and Py/Py binds both A•T and T•A. Exploitation of polyamides to target sequences of biological interest has yielded results in a number of cell-free systems.[3-8]

Extension of these *in vitro* biological results to cellular systems has proven to be cell-type dependent. Polyamides exhibited biological effects in primary human lymphocytes,[9] human cultured cell lines,[10] and when fed to *Drosophila* embryos.[11,12] However, attempts to inhibit the transcription of endogenous genes in cell lines other than insect or T-lymphocytes have met with little success. For example, polyamides that down-regulate transcription of the HER2/*neu* gene in cell-free experiments display no activity in HER2-overexpressing SK-BR-3 cells.[13]

To determine if these results were due to poor cellular uptake or nuclear localization, a series of polyamides incorporating the fluorophore Bodipy FL was synthesized. Intracellular distribution of these molecules in several cell lines was then

determined by confocal laser scanning microscopy.[14] Cells which demonstrated robust responses to polyamides, such as T-lymphocyte derivatives, showed staining throughout the cells, including the nucleus. In other cell lines studied, however, treatment with polyamide-Bodipy conjugates produced a punctate staining pattern in the cytoplasm, with no observable signal in the nuclei. Bashkin and coworkers recently reported that an eight-ring polyamide-Bodipy conjugate colocalized with LysoTracker Red DND 99 (a lysosome and *trans*-Golgi stain, **23**) in several cell lines, indicating that the punctate staining pattern was presumably due to trapping of the polyamide in acidic vesicles.[15] In contrast, an eight-ring polyamide-fluorescein conjugate, **1**, was shown to accumulate in the nuclei of HCT-116 human colon cancer cells.

We have found that a similar eight-ring polyamide-fluorescein conjugate, **2**, with a single Py to Im change, is excluded from the nuclei of thirteen different mammalian cell lines, whereas removal of the β-Ala residue in the linker, affording **3**, enables nuclear localization in all of these cell lines, with no obvious toxicity. This raises the issue: what are the molecular determinants—fluorophore, position of attachment, linker composition, polyamide sequence and size—of uptake and nuclear localization in cultured cells? Understanding nuclear accessibility in a wide variety of living cells is a minimum first step toward chemical regulation of gene expression with this class of molecules. A further issue will be whether polyamides modified for optimal cellular and nuclear uptake retain favorable DNA-binding affinity and sequence specificity. We have synthesized twenty-two polyamide-fluorophore conjugates with incremental changes in structure and examined their intracellular distribution in thirteen cell lines.

Results

Structures for all of the compounds synthesized are listed in Figure 4.1. Sample images for compounds **2** and **3** in two cell lines are shown in Figure 4.2a. To show that compound **3** localizes to the nuclei of live cells, samples were treated with **3**, the nuclear stain Hoechst 33342, and the dead-cell stain Sytox Orange (Figure 4.2b). The uptake characteristics of compounds **1-22** were examined in thirteen cell lines by confocal microscopy, and each sample was rated qualitatively for the extent of nuclear localization (Figure 4.3).

The molecules showing the highest degree of nuclear uptake in most cell lines stained nuclei very brightly with reference to the background fluorescence caused by fluorescent agent in the medium. Agents **1**, **3**, **5**, **6**, **11-14**, and **22** showed such high levels of uptake in many cell lines. Many compounds exhibited a very scattered uptake profile in the series of cells studied, and compounds **2**, **4**, **15**, and **21**, showed no significant nuclear staining in any cell line. Of the entries in Figure 4.3 indicating poor nuclear uptake properties, most reflect lysosomal staining, as indicated by costaining with LysoTracker Red DND-99, as well as fluoresence in the intercellular medium. Only compound **2** was found exclusively in the medium, showing no uptake in cells.

The DNA-binding properties of **3** were assessed by DNase I footprinting titrations on the plasmid pDEH9, which bears the 5'-TGGTCA-3' match site and discrete single base-pair mismatch sites. Conjugate **3** bound to the match site with a K_a of 1.6 ($\pm$ 0.3) x 10^9 M^{-1}, and showed specificity over mismatch sites by >100-fold (Figure 4.4).

To investigate the energy dependence of the cellular uptake mechanism of compound **3**, HeLa cells growing under normal conditions were incubated for 30 min in
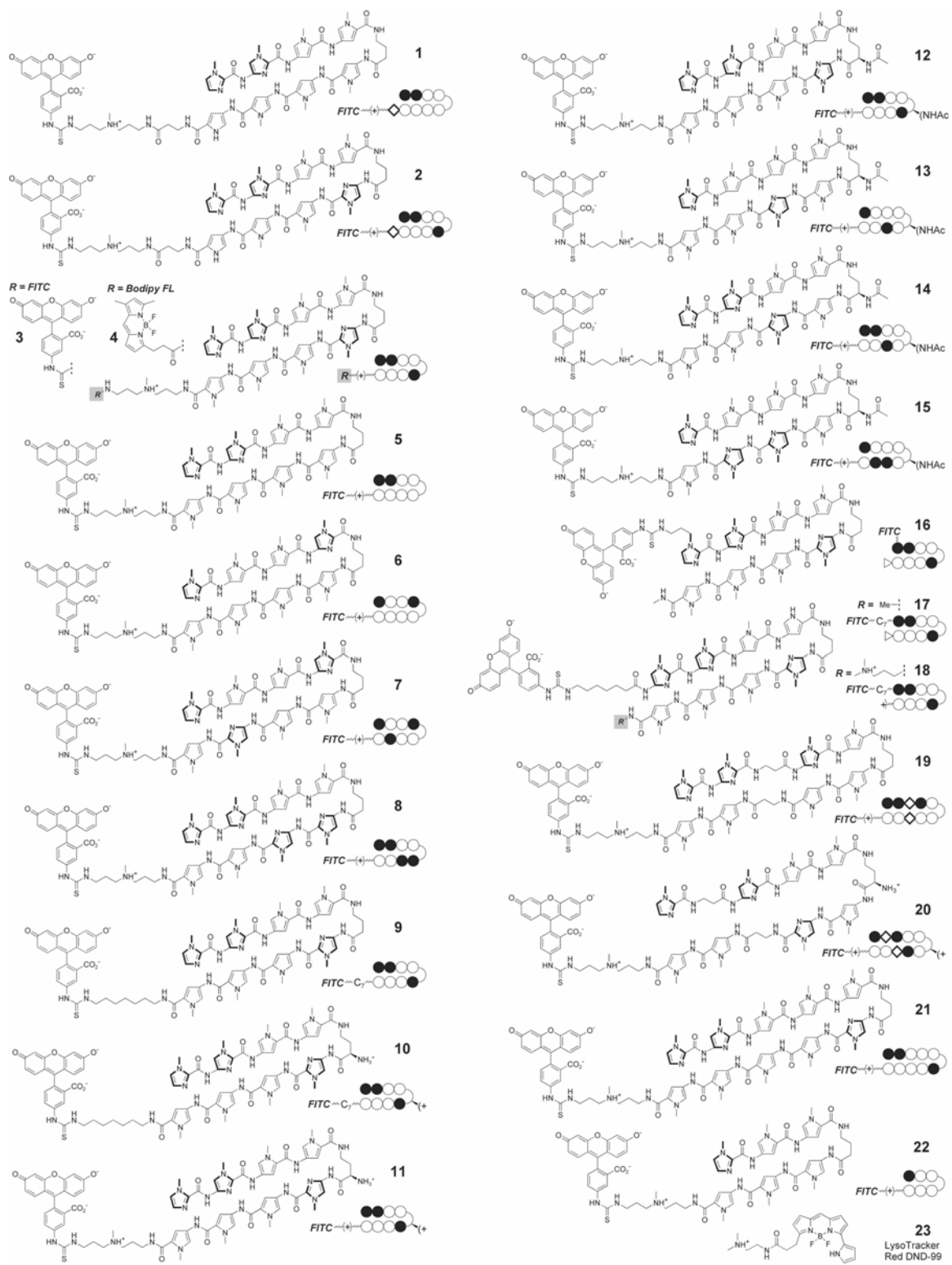
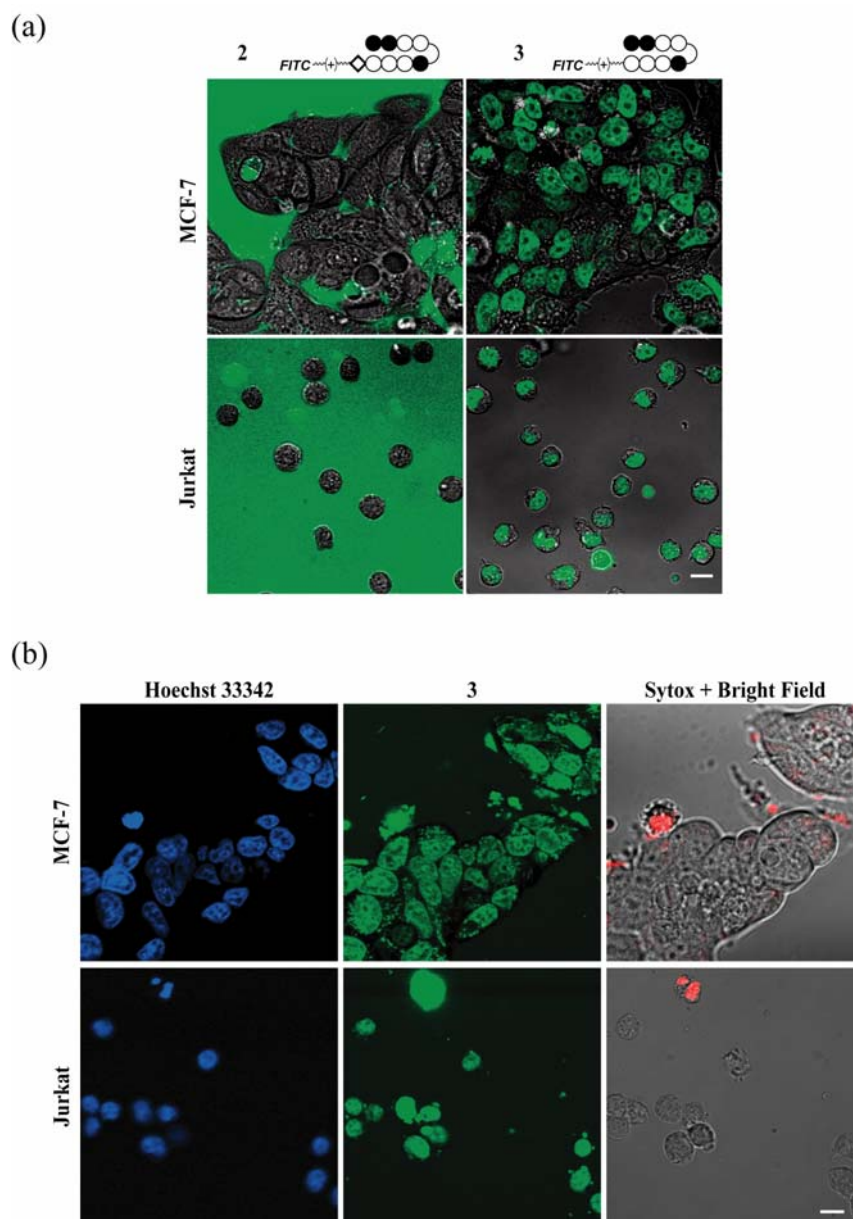**Figure 4.1** Structures of compounds used in uptake experiments.

Figure 4.2 Cellular localization of polyamide-fluorescein conjugates. (a) (*Top*) Adherent MCF-7 cells were treated with compound **2** (*Upper left*) or **3** (*Upper right*) for 10-14 h at 5 μM. Compound **2** was excluded from the cells entirely, while compound **3** localized to the nucleus. (*Bottom*) Suspended Jurkat cells were similarly treated, and show similar results. (b) Colocalization of polyamide **3** and Hoechst in live cells, imaged using sequential single- and two-photon excitation. (*Top*) MCF-7 cells were treated with the nuclear stain Hoechst 33342 (15 μM), compound **3** (5 μM), and the dead cell stain Sytox Orange (0.5 μM). Fluorescence signals from Hoechst (*Upper left*, blue) and compound **3** (*Upper center*, green) colocalize in cell nuclei. (*Upper right*) Overlay of the visible light image (grayscale) and the Sytox Orange fluorescence image (red), indicating that the majority of cells are alive. (*Bottom*) Jurkat cells were treated similarly, and show similar results. (Scale bar = 10 μm.)
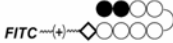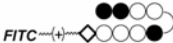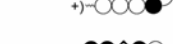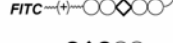
Compound	DLD-1	HeLa	MCF-7	SK-BR-3	786-O	293	LN-CaP	PC3	MEL	NB4	Jurkat	CCRF-CEM	MEG-01
1	+	++	++	++	+	+	++	++	+	++	++	++	++
2	−	−−	−−	−−	−−	−−	−−	−−	−−	−−	−−	−−	−−
3	+	++	++	++	++	++	++	++	++	++	++	++	++
4	−	−	−	−	−−	−−	−−	−	−	−	−	−−	−
5	++	++	++	++	++	++	++	++	++	++	++	++	++
6	++	++	++	++	++	++	++	++	++	++	++	++	++
7	+	++	+	+	+	+	+	+	−−	−	++	++	+
8	−	+	+	−	−−	−	−	−	−−	−−	−−	−	−−
9	−	−−	+	+	−−	−−	−	−−	−−	−−	−	−	−−
10	+	++	+	+	+	−−	++	+	+	+	++	+	+
11	+	++	+	+	+	++	++	++	+	−−	++	+	++
12	++	++	++	++	++	++	++	++	++	++	++	++	++
13	++	++	++	++	++	++	++	++	++	+	++	++	++
14	++	++	++	++	+	++	++	++	+	−	++	++	++
15	−−	−−	−−	−−	−	−−	−−	−−	−−	−−	−−	−−	−−
16	+	−−	+	+	−−	−	−−	−	−−	−	+	−	−−
17	+	−	++	+	−−	−−	−−	+	+	+	+	+	+
18	+	++	++	+	−	+	−	+	++	−	++	+	+
19	−	+	−	+	−	−−	+	+	+	++	−	−−	+
20	−	++	+	−	+	−	+	+	−−	−−	+	+	+
21	−	−	−−	−	−−	−−	−	−−	−−	−−	−−	−−	−−
22	++	++	++	++	++	++	++	++	++	++	++	++	++

Figure 4.3 Uptake profile of compounds **1-22** in 13 cell lines: "+ +" Indicates nuclear staining exceeds that of the medium; "+" indicates nuclear staining ≤ that of the medium, but still prominent; "-" indicates very little nuclear staining, with the most fluorescence seen in the cytoplasm and/or medium; "--" indicates no nuclear staining.
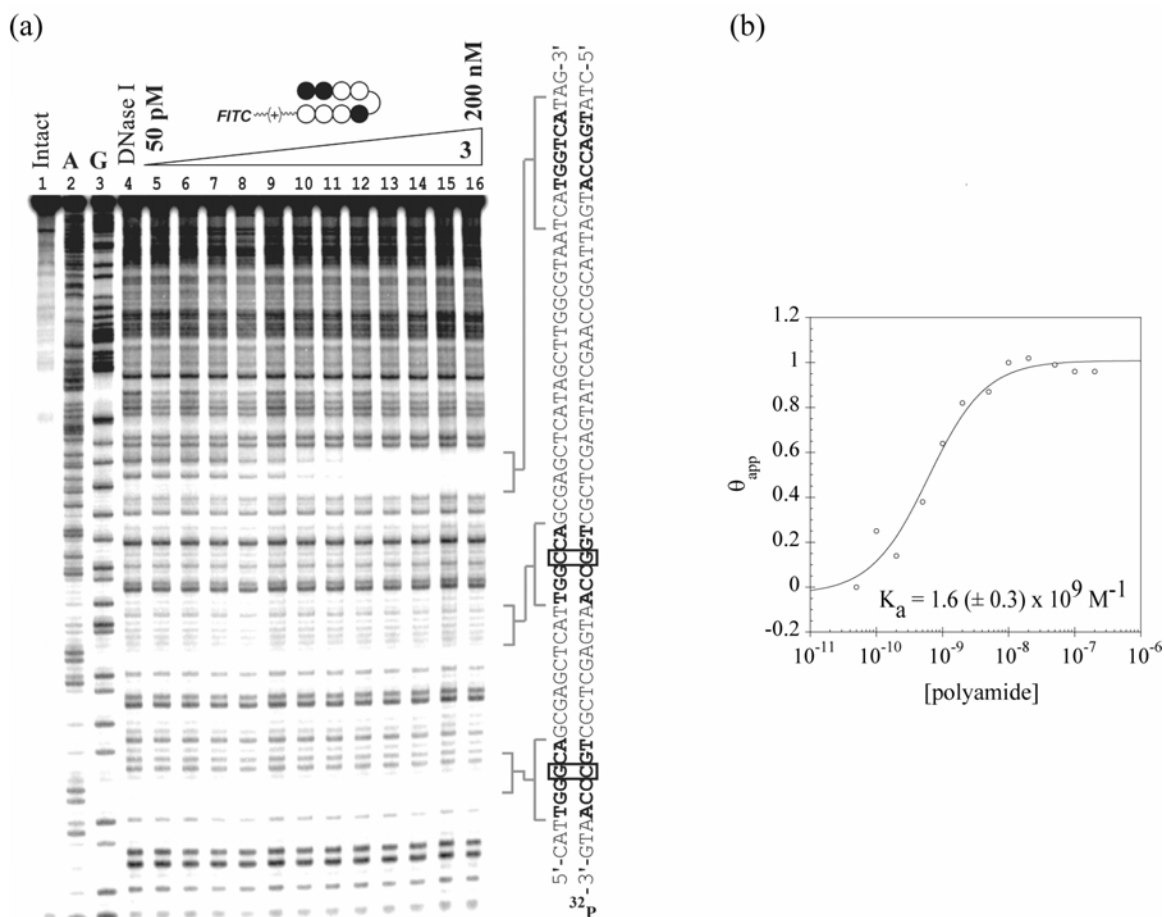
Figure 4.4 Quantitative DNase I footprinting titration. (a) Compound **3** binds the 3'-TGGTCA-5' site with an affinity $K_a = 1.6 \ (\pm 0.3) \times 10^9 \ M^{-1}$. Compound **3** does not bind the single base-pair mismatch sites shown at concentrations ≤ 200 nM. (b) DNA binding isotherm for compound **3**.

either normal DMEM medium or inhibitory DMEM medium, then treated with **3** for 1 hr prior to confocal imaging (Figure 4.5). The cells growing in normal medium showed clear nuclear staining, whereas the cells growing in inhibitory medium displayed very little to no discernable staining. Subsequent washing and replacement of the inhibitory medium with normal medium (supplemented with 5 μM **3**), resulted in nuclear staining after 1 h, comparable to that seen in the sample grown continuously in the normal medium.

It had been shown previously that polyamide-Bodipy conjugates stain the nuclei of T-lymphocytes, but no other cell type tested, and most commonly produced a punctate cytoplasmic staining pattern.[14] Our studies indicated that a polyamide-fluorescein conjugate, **2**, uniformly proved refractory to nuclear uptake in several human cancer cell lines. Elimination of the β-alanine residue at the carboxy-terminal end of the polyamide afforded compound **3**, which, surprisingly, showed excellent nuclear staining properties in the cell lines examined. Attachment of the Bodipy-FL fluorophore to the polyamide precursor of compound **3** provided compound **4**. This molecule showed no nuclear staining, sequestering itself in cytoplasmic vesicles, indicating that some characteristic of polyamide-Bodipy conjugates differing from that of polyamide-FITC conjugates, and not the C-terminal β-alanine, prevents their trafficking into the nucleus. It is interesting to note that the structure of LysoTracker Red DND-99 (**23**) includes both a tertiary alkyl amine, similar to that often used in hairpin polyamide tails, and a Bodipy moiety.

It became our intent to explore the structure-space of polyamide-fluorophore conjugates to overcome cellular exclusion and lysosomal trapping, allowing the polyamides to travel to the nucleus. To explore the criteria that permit uptake of **3**, and
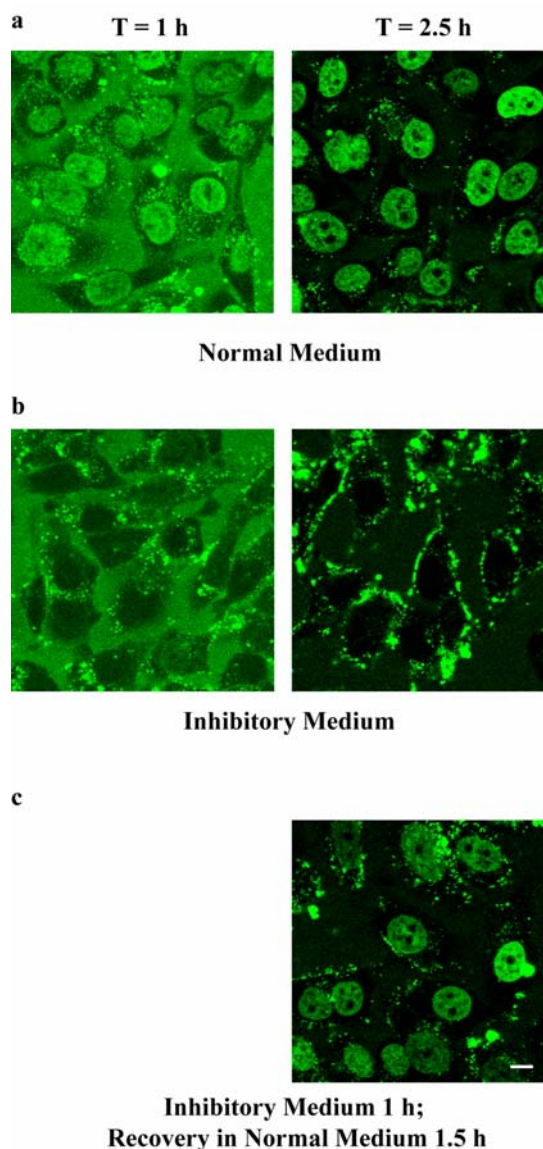
Figure 4.5 Energy dependence of nuclear localization of compound **3**. (a) HeLa cells were washed, incubated in normal DMEM medium for 30 min, supplemented with 5 mM **3**, incubated for 1 h, and imaged, showing roughly equivalent amounts of compound localized both in the nucleus and in the medium (*left*). The cells were incubated for a further 1 h 30 min, and then imaged once more (*right*), showing exclusively nuclear localization. (b) HeLa cells were washed, incubated in inhibitory DMEM medium for 30 min, supplemented with 5 mM **3**, incubated for 1 h, and imaged, showing localization at the cellular membranes, as well as in the medium (*left*). The cells were incubated for a further 1 h 30 min, and then imaged once more (*right*), showing exclusively membranous localization. (c) Recovery experiment: HeLa cells treated as in b were washed 2x with normal DMEM medium, incubated for 1h 30 min in normal DMEM medium supplemented with 5 mM **3**, then imaged, showing recovery of nuclear localization upon replacement of inhibitory medium with normal medium. (Scale bar = 10 μm.)

that prevent that of **4**, several variations on the structure of the compound were made and their effects determined by confocal microscopy.

Wishing to explore the effect of Py/Im sequence and content of hairpin polyamides on cellular trafficking, we synthesized compounds **5-8**. Compounds **5** and **6**, both containing two imidazole residues, showed a high degree of nuclear staining in all cell lines studied. Three-imidazole compound **7** showed intermediate levels of nuclear staining in the cell lines studied. The nuclear localization of four-imidazole compound **8** was quite poor in all cell lines tested. The difference in nuclear staining levels exhibited by compounds **3** and **7** shows that Py/Im sequence alone is an important determinant of nuclear uptake, though overall content (in terms of the number of Py and Im residues) may also be a factor.

To explore the effect of the positively-charged linker on nuclear uptake, compound **9** was synthesized. This agent showed nearly global abrogation of nuclear uptake efficiency versus the analog containing a tertiary amine. Further, substitution of the γ-aminobutyric acid turn (γ-turn) of **9** with the [(R)-α-amino]-γ-diaminobutyric acid turn (^{H_2N}γ-turn) provided **10**, which restored most of the nuclear uptake properties of **3**. This suggests that the overall charge of the molecule, and perhaps the placement of that charge, are important variables in nuclear uptake of polyamide-dye conjugates.

The ^{H_2N}γ-turn is a structural element commonly included in polyamide design. Replacement of the γ-turn of **3** with the ^{H_2N}γ-turn provided **11**. This molecule showed nuclear staining in all cell lines tested, save NB4, though often to a lesser degree than **3**. It is unclear whether this reduction in uptake efficiency is due to an increase in the overall

positive charge of the molecule, a more branched structure than the linear γ-linked hairpin, or the positioning of a positive charge medial in the molecule.

Selective acetylation of the polyamide precursor to **11**, followed by FITC conjugation, provided **12**. This molecule exhibited excellent nuclear uptake, as good or better than both **11** and **3**. The excellent uptake of **12** argues against branching as a negative determinant of nuclear staining. This result also prompted us to synthesize **13-15** to probe the generality and flexibility of turn acetylation across several polyamide sequences. The uptake of **13** and **14** was mostly nuclear. Compound **15**, on the other hand, was a very poor nuclear stain. This result reaffirms the importance of polyamide sequence on nuclear uptake.

We next synthesized several conjugates to explore the uptake effects of different points of attachment of the fluorophore-linker moiety to the polyamide. An *N*-propylamine linkage from the terminal imidazole and a methylamide tail were incorporated into **16**, which showed poor nuclear uptake in nearly all cell lines tested. We thought it possible that the poor uptake properties of conjugate **16** was due to some non-linearity introduced into the overall structure of the molecule by the linkage at the 1-position of the N-terminal ring of the polyamide. Consequently, conjugates **17** and **18** were synthesized, appending the linker-fluorophore moiety to the N-terminal amine. Although compound **17** has an overall structure and charge distribution very similar to that of **9**, it possesses better nuclear uptake properties, particularly in suspended cell lines. Subsequent addition of a positive charge at the C-terminal end of the polyamide through employment of an *N,N*-dimethylaminopropylamine tail (compound **18**) boosts uptake in all cell lines studied, save NB4. Once again, this suggests that the addition or deletion of

a single charge may (but not necessarily will) have a strong effect on nuclear uptake. In fact, a comparison of compounds **3**, **10**, and **18** (differing in the placement of a positive charge) with **9** and **17** (which lack a positive charge) seems to indicate that the positioning of this charge is less influential than its presence.

Another common structural feature utilized in DNA-binding polyamides is the addition of one or more β-alanine residues. This amino acid is often used to relax overcurvature of a polyamide backbone with reference to the minor groove of DNA and permits the targeting of longer sequences than that of eight-ring hairpins. Compound **19**, which includes this structural element, and **20**, which includes both β-alanines and the ^{H_2N}γ-turn, showed fair to poor nuclear uptake in the cell line series. The reduced uptake levels could be due to the increased molecular flexibility imparted by the β-alanine residues, increased molecular weight, decreased recognition by a cellular import protein, or some combination of these criteria.

In order to determine whether or not the added size imparted to **19** and **20** by the β-alanine residues was likely a major contributor to their poor uptake, the ten-ring compound **21** was synthesized. Its ubiquitously poor nuclear uptake suggests that molecular weight may, indeed, play a prominent role in uptake character. The excellent uptake character of the six-ring compound **22** furthers this hypothesis, though Py/Im sequence in the 6-ring and 10-ring contexts is also likely to be important.

This study demonstrates the cellular localization profile of a host of polyamide-dye conjugates in a wide variety of cell lines. In general, compounds exhibiting good nuclear uptake properties have several common elements: an eight-ring polyamide DNA-binding domain, one or more positive charges incorporated within either the linker or the

turn residue, and a conjugated fluorescein fluorophore. This study also demonstrates that each cell line possesses a unique uptake profile for the panel of compounds presented to it. These profiles will be important in choosing a cell line and compound architecture appropriate to a given experiment.

Conjugation of the fluorophore to the polyamide DNA-recognition domain results in an approximately 10-fold reduction in DNA-binding affinity as compared with the parent polyamide, with retention of binding specificity over mismatch sites. This quality, along with the nuclear uptake results, suggests that fluorophore-conjugated polyamides may be employed directly in experiments designed to take place in living mammalian cells.

Clearly, there are many criteria at work, each one having its share of influence upon nuclear uptake of polyamide-dye conjugates. The extension of the structure-space of compounds known to both bind chromosomal DNA specifically and with high affinity, as well as to traffic to the nucleus of living cells is the object of current investigations. The illumination of these possibilities will permit the further study of transcriptional regulation in living systems.

Experimental

Chemicals

Polyamides **1** and **2** were prepared by solid-phase methods on Boc-β-alanine-PAM-resin (Peptides International; Louisville, KY).[16] All other polyamides were synthesized by solid phase methods on the Kaiser oxime resin (Nova Biochem; Laufelfingen, Switzerland).[17] After cleavage with the appropriate amine and reverse-

phase HPLC purification, polyamides were allowed to react at room temperature for ~3 h at ~0.01 M in *N,N*-dimethylformamide with fluorescein isothiocyanate (FITC; compounds **1-3** and **5-22**) or the *N*-hydroxysuccinimidyl ester of BODIPY-FL (**4**), as well as 20 eq of Hünig's base, to yield polyamide-dye conjugates. The purity and identity of the dye conjugates were verified by analytical HPLC, UV-vis spectroscopy and MALDI-TOF mass spectrometry. All fluorescent dye reagents were from Molecular Probes. Chemicals not otherwise specified were from Aldrich.

Mass Spectra

MALDI mass spectra were obtained on a Voyager De PRO time-of-flight mass spectrometer (Applied BioSystems) operated at an accelerating voltage of +20 kV. Samples were applied to the target in an α-cyanohydroxycinnamic acid matrix. The mass spectrometer was calibrated with a calibration mixture provided by the instrument manufacturer. The mass spectra data are summarized in Table 4.1.

Preparation of Polyamide Solutions

To make 100 μM solutions of each compound, dry HPLC-purified aliquots of each conjugate were dissolved to 1-10 mM in DMSO, then diluted with PBS buffer (pH 7.4) or 18 MΩ cm water to ~200 μM. A small portion of this solution was diluted to ~10 μM and the concentration determined by UV quantitation at 310 nm (compounds **1-20**: ε = 69500; compound **21**: ε = 86875; compound **22**: ε = 52125) the concentrated solution was then diluted to 100 μM. The final concentration of DMSO in any sample was less than 1.5%, usually less than 0.1%.

Cell Cultures

The human cancer cell lines DLD-1, MCF-7, 786-O, LNCaP, PC3, MEG-01, NB4, Jurkat, and CCRF-CEM were cultured in a 5% CO_2 atmosphere at 37°C in supplemented RPMI-1640 medium.   The human cancer cell line HeLa, the murine leukemia cell line MEL, and the transformed human kidney cell line 293 were grown as above in supplemented Dulbecco's Modified Eagle medium (DMEM).   The human cancer cell line SK-BR-3 was cultured as above in supplemented McCoy's medium.   All media were supplemented with 10% fetal bovine serum (Irvine Scientific) and 1% penicillin/streptomycin solution (Sigma).

Confocal Microscopy

Adherent cell lines were trypsinized for 5-10 min at 37°C, centrifuged for 5 min at 5°C at 2000 rpm, and resuspended in fresh medium to a concentration of 1.25 x 10^6 cells/mL. Suspended cell lines were centrifuged and resuspended in fresh medium to the same concentration. Incubations were performed by adding 150 μL cells into culture dishes equipped with glass bottoms for direct imaging (MatTek Corporation). Adherent cells were grown in the glass-bottom culture dishes for 24 h. The medium was then removed and replaced with 142.5 μL of fresh medium. Then 7.5 μL of the 100 μM polyamide solution was added and the cells were incubated in a 5% CO_2 atmosphere at 37°C for 10-14 h. Suspended cell line samples were prepared in a similar fashion, omitting trypsinization. These samples were then incubated as above for 10-14 h. Imaging was performed with a Zeiss LSM 5 Pascal inverted laser scanning microscope.

Images were line-averaged 4, 8, or 16 times and were obtained at a 0.8 μs/pixel scanning rate.   Polyamide-fluorescein conjugate fluorescence and visible light images were obtained using 488 nm laser excitation with a standard fluorescein filterset and a pinhole of 181 μm.   For two-color experiments with LysoTracker Red DND-99, cells were treated with 0.75 μL of a 100 μM DMSO stock solution, affording a final dye concentration of 500 nM LysoTracker.   After ~10 min incubation with LysoTracker, images were obtained by simultaneous 488 nm and 543 nm laser excitation and a filterset appropriate for simultaneous visualization of fluorescein and rhodamine.

Hoechst colocalization experiments were performed on a Zeiss LSM 510 META NLO upright laser scanning microscope with a Coherent Chameleon 2-photon laser.   For the MCF-7 cell line, the cells were grown in glass-bottom culture dishes in a volume of 150 μL and treated with polyamide **3** as usual.   Approximately 30 min prior to imaging, 0.75 μL of Sytox Orange solution (100 μM in DMSO) and 3 μL of Hoechst 33342 solution (750 μM in sterile water) were added to the cell medium, affording final dye concentrations of 500 nM Sytox and 15 μM Hoechst.   Immediately prior to imaging, a coverslip was placed over the cells, and the dish inverted.   Three sequential images were obtained in succession, at a 0.8 μs/pixel scanning rate.   The images were line-averaged 8 times.   The Sytox and visible light overlay was collected using 543 nm laser excitation with a standard rhodamine filterset and a pinhole of 499 μm.   The polyamide-fluorescein conjugate was imaged using 488 nm laser excitation with a standard fluorescein filterset and a pinhole of 181 μm.   Hoechst was imaged using 800 nm laser two-photon excitation with an HFT KP 680 dichroic and a 390-465 nm bandpass filter with a fully open pinhole.

For the Jurkat cell line, cells were treated as above, but immediately prior to imaging, 30 μL of the cell solution was placed between a clean glass slide and a coverslip separated by a coverslip spacer. Images were collected in multitrack mode, at a 0.64 μs/pixel scanning rate. The images were line-averaged 8 times. Sytox and Hoechst were imaged using 800 nm laser two-photon excitation with an HFT KP 680 main dichroic, an NFT 545 secondary dichroic, a 565-615 nm bandpass filter for the Sytox signal (fully open pinhole), and a 390-465 bandpass filter for the Hoechst signal (363 μm pinhole). The polyamide-fluorescein conjugate and visible light images were obtained using 488 nm laser excitation with a standard fluorescein filterset and a pinhole of 249 μm.

Energy Dependence Experiments

Inhibitory medium was prepared by supplementing glucose- and sodium pyruvate-free DMEM (Gibco #1196025) with 2-deoxyglucose (6 mM) and sodium azide (10 mM).[18] Cells were grown, trypsinized, resuspended, plated and incubated as above. After 24 h of growth at 37°C in 5% CO_2, the medium was removed and replaced with either 142.5 μL fresh normal DMEM medium or 142.5 μL inhibitory DMEM medium. The cells were incubated for 30 min, then treated with 7.5 μL of 100 μM compound **3**. The cells were then incubated for 1 h, followed by confocal imaging as above. Samples in inhibitory medium were then treated by removal of the medium, washing and removal of 200 μL of normal medium, replacement with 142.5 μL of normal medium and addition of 7.5 μL of 100 μM compound **3**. These samples were incubated for 1 h and then imaged once more.

DNase I Footprinting Titration Experiments

A 3'-[^{32}P]-labeled restriction fragment from the plasmid pDEH9 was generated in accordance with standard protocols and isolated by nondenaturing gel electrophoresis.[19,20]

1	H-FITC	1265.6	1265.8
2	H-FITC	1266.6	1267.3
3	H	1584.6	1584.5
4	Na	1490.7	1490.7
5	H	1583.6	1583.6
6	H-FITC	1194.6	1194.6
7	H	1584.6	1585.1
8	H	1585.6	1585.2
9	H	1569.6	1569.6
10	H	1584.6	1584.7
11	H-FITC	1210.6	1210.6
12	H	1641.6	1641.5
13	H	1640.6	1641.4
14	H	1641.6	1642.4
15	H	1641.6	1641.5
16	H	1513.5	1513.3
17	H	1634.6	1634.4
18	H-FITC	1294.6	1294.8
19	H	1797.7	1797.9
20	H	1812.7	1812.8
21	H –FITC	1461.7	1461.8
22	H	1339.5	1339.6

Table 4.1 Mass spectra for compounds **1-22**.

Acknowledgements

References

1)   Dervan, P.B.; Edelson, B.S. *Curr. Opin. Struct. Biol.* **2003,** *13*, 284.

2)   Dervan, P.B. *Bioorg. Med. Chem.* **2001**, *9*, 2215.

3)   Dickinson, L.A.; Trauger, J.W.; Baird, E.E.; Ghazal, P.; Dervan, P.B.; Gottesfeld, J.M. *Biochemistry* **1999**, *38*, 10801.

4)   Gottesfeld, J.M.; Turner, J.M.; Dervan, P.B. *Gene Expression* **2000**, *9*, 77.

5)   Wang, C.C.C.; Dervan, P.B. *J. Am. Chem. Soc.* **2001**, *123*, 8657.

6)   Ansari, A.Z.; Mapp, A.K.; Nguyen, D.H.; Dervan, P.B.; Ptashne, M. *Chem. Biol.* **2001**, *8*, 583.

7)   Gottesfeld, J.M.; Melander, C.; Suto, R.K.; Raviol, H.; Luger, K.; Dervan, P.B. *J. Mol. Biol.* **2001**, *309*, 615.

8)   Ehley, J.A.; Melander, C.; Herman, D.; Baird, E.E.; Ferguson, H.A.; Goodrich, J.A.; Dervan, P.B.; Gottesfeld, J.M. *Mol. Cell. Biol.* **2002**, *22*, 1723.

9)   Dickinson, L.A.; Gulizia, R.J.; Trauger, J.W.; Baird, E.E.; Mosier, D.E.; Gottesfeld, J.M.; Dervan, P.B. *Proc. Natl. Acad. Sci. U.S.A.* **1998**, *95*, 12890.

10)   Coull, J.J.; He, G.C.; Melander, C.; Rucker, V.C.; Dervan, P.B.; Margolis, D.M. *J. Virol*. **2002**, *76*, 12349.

11)   Janssen, S.; Durussel, T.; Laemmli, U.K. *Mol. Cell* **2000**, *6*, 999.

12)   Janssen, S.; Cuvier, O.; Muller, M.; Laemmli, U.K. *Mol. Cell* **2000**, *6*, 1013.

13)   Chiang, S.Y.; Bürli, R.W.; Benz, C.C.; Gawron, L.; Scott, G.K.; Dervan, P.B.; Beerman, T.A. *J. Biol. Chem*. **2000**, *275*, 24246.

14)   Belitsky, J.M.; Leslie, S.J.; Arora, P.S.; Beerman, T.A.; Dervan, P.B. *Bioorg. Med. Chem.* **2002**, *10*, 3313.

15)   Crowley, K.S.; Phillion, D.P.; Woodard, S.S.; Schweitzer, B.A.; Singh, M.; Shabany, H.; Burnette, B.; Hippenmeyer, P.; Heitmeier, M.; Bashkin, J.K. *Bioorg. Med. Chem. Lett*. **2003**, *13*, 1565.

16)   Baird, E.E.; Dervan, P.B. *J. Am. Chem. Soc*. **1996**, *118*, 6141.

17)   Belitsky, J.M.; Nguyen, D.H.; Wurtz, N.R.; Dervan, P.B. *Bioorg. Med. Chem*. **2002**, *10*, 2767.

18)   Richardson, W.D.; Mills, A.D.; Dilworth, S.M.; Laskey, R.A.; Dingwall, C. *Cell* **1998**, *52*, 655.

19)   Heckel, A.; Dervan, P.B. *Chem. Eur. J*. **2003**, *9*, 3353.

20)   Trauger, J.W.; Dervan, P.B. *Methods Enzymol*. **2001**, *340*, 450.